frontiers | Frontiers in Physics

TYPE Original Research
PUBLISHED 24 April 2023
DOI 10.3389/fphy.2023.1178257

Check for updates

OPEN ACCESS

EDITED BY
Changbo Fu,
Fudan University, China

REVIEWED BY
Zhao Yongtao,
Xi'an Jiaotong University, China
Yangping Shen,
China Institute of Atomic Energy, China

*CORRESPONDENCE
X. Q. Yan,
x.yan@pku.edu.cn

RECEIVED 02 March 2023
ACCEPTED 12 April 2023
PUBLISHED 24 April 2023

CITATION
Wu D, Lan HY, Zhang JY, Liu JX, Lu HG, Lv JF, Wu XZ, Zhang H, Cai J, Xu XL, Geng YX, Ma WJ, Lin C, Zhao YY, Wang HR, Liu FL, He CY, Yu JQ, Guo B, Wang NY and Yan XQ (2023), New measurements of ^{92}Mo(γ, n) and (γ, 3n) reactions using laser-driven bremsstrahlung γ-ray.
Front. Phys. 11:1178257.
doi: 10.3389/fphy.2023.1178257

New measurements of ^{92}Mo(γ, n) and (γ, 3n) reactions using laser-driven bremsstrahlung γ-ray

D. Wu[1,2], H. Y. Lan[1,2], J. Y. Zhang[1,2], J. X. Liu[1,2], H. G. Lu[1,2], J. F. Lv[1,2], X. Z. Wu[1,2], H. Zhang[1,2], J. Cai[1,2], X. L. Xu[1,2], Y. X. Geng[1,2], W. J. Ma[1,2], C. Lin[1,2], Y. Y. Zhao[1,2], H. R. Wang[3], F. L. Liu[3], C. Y. He[3], J. Q. Yu[4], B. Guo[3], N. Y. Wang[3] and X. Q. Yan[1,2]*

[1]State Key Laboratory of Nuclear Physics and Technology, School of Physics, CAPT, Peking University, Beijing, China, [2]Beijing Laser Acceleration Innovation Center, Beijing, China, [3]Department of Nuclear Physics, China Institute of Atomic Energy, Beijing, China, [4]School of Physics and Electronics, Hunan University, Changsha, China

The flux-weighted average cross sections and isomeric ratios of ^{92}Mo(γ, n)^{91m,g}Mo and ^{92}Mo(γ, 3n)^{89}Mo reactions were measured through activation methods. Laser-driven bremsstrahlung γ-ray were generated by the laser wakefield accelerated quasi-monoenergetic electrons using the 200 TW laser in the Compact Laser Plasma Accelerator laboratory, Peking University. The results showed good agreements with previous works using traditional γ-ray sources, and were compared with TALYS 1.9 calculations. We extended the experimental results of ^{92}Mo photonuclear reactions to higher energies, the experimental discrepancies of ^{92}Mo(γ, n)^{91m,g}Mo isomeric ratios at high energy region were clarified, and the cross sections of ^{92}Mo(γ, 3n)^{89}Mo reaction were first obtained.

KEYWORDS
^{92}Mo(γ, n)^{91m,g}Mo, ^{92}Mo(γ,3n)^{89}Mo, photonuclear reaction, flux-weighted average cross section, isomeric ratio, laser-driven γ-ray

1 Introduction

With the rapid developments of laser electron accelerations, especially laser wakefield accelerations (LWFA) [1–7], laser-driven γ-ray can reach an extremely high intensities of 10^{22-24} s^{-1} [8–12], which are several orders of magnitude stronger than other γ-ray sources such as laser Compton scattering (LCS) [13, 14] or electron linac bremsstrahlung [15]. Researchers have shown considerable interests in laser-induced nuclear reactions in nuclear physics such as photonuclear studies [16, 17], photon fission [16, 18] and photon activation analysis [19].

Photonuclear reaction cross sections and their isomeric ratios (IR) play a significant role in nuclear structure, nuclear reaction mechanism, and nuclear astrophysics [20–22]. The IRs of a nuclear reaction were a powerful tool for testing nuclear structure theories and nuclear reaction models [20, 21, 23, 24]. In nuclear astrophysics, there are 30–35 proton-rich nuclei (*p*-nuclei) that can only be produced by *p*-processes [25–28]. The production mechanisms of *p*-nuclei contain a series of photonuclear reactions [29]. The experimental measurements of those reactions are vital for nuclear synthesis and stellar models [29]. Recently, Wu *et al.* successfully measured the flux-weighted average cross sections (FACS) and IRs of ^{197}Au(γ, *xn*; *x* = 1~7) reactions using a 200TW laser facility [30]. Their results demonstrated that the

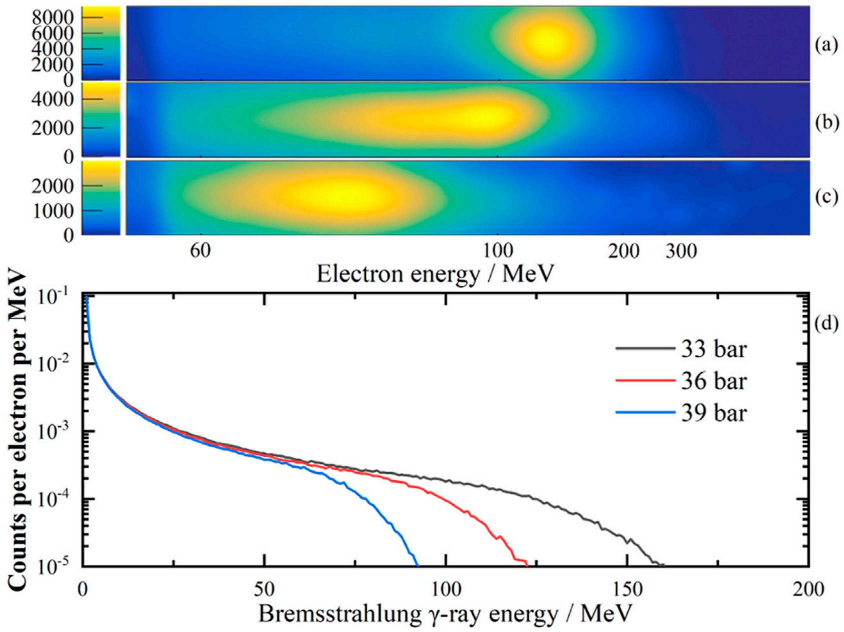

FIGURE 1
(A–C) are the typical LWFA electron spectra obtained by the magnetic spectrometer at gas pressure of 33, 36, 39 bar, respectively. **(D)** is the bremsstrahlung γ-ray energy spectra obtained from GEANT4 simulations using the averaged electron spectra of 100 continuous shots.

accuracy of laser-driven γ-rays is sufficient for photonuclear reaction cross section and IR measurements.

^{92}Mo, one of the light p-nucleus pair ^{92,94}Mo [29], is a well known even-even nuclei with a spin of 0 and a neutron number of 50. For ^{92}Mo(γ, n)^{91}Mo reaction, ^{91}Mo can be formed with the isomeric state with a spin of 1/2$^-$ or the ground state with a spin of 9/2$^+$. A lot of works had reported the cross sections [31–33] and IRs [31, 34–39] of ^{92}Mo(γ, n)^{91m,g}Mo reaction, but the experimental IRs did not match each other very well, especially at high energy region. In the giant dipole resonance (GDR) region, Thiep *et al.* [39] and Davidov *et al.* [37] had a maximum difference of 26%. In high energy region, Bartsch *et al.* [38] reported an IR of 0.97 at end-point energy of 55 MeV while Haustein *et al.* [35] measured an IR of 0.52 at end-point energy of 70 MeV, the huge difference is quite doubtful for high-energy IRs. For ^{92}Mo(γ, 3n)^{89}Mo reaction, no experimental cross section data are available for now.

In this study, we used laser-driven bremsstrahlung γ-rays to measure the FACSs and IRs of ^{92}Mo(γ, n)^{91m,g}Mo reaction. The discrepancies of ^{92}Mo(γ, n)^{91m,g}Mo IRs at high energy region were clarified. Meanwhile, the ^{92}Mo(γ, 3n)^{89}Mo reaction cross sections were first achieved.

2 Experiment

2.1 Accelerator

The experiments were performed at the 200 TW laser facility in the Compact Laser Plasma Accelerator (CLAPA) Laboratory, Peking University. The facility delivers 4 J, 30 fs, 5 Hz laser pulses in the center wavelength of 800 nm. 60~250 MeV monoenergetic electrons were generated in LWFA by focusing the laser with a focal length of 100 cm on a supersonic nozzle. A 2 mm Ta (99.9%) disk was used as a bremsstrahlung converter. More details can be found in our previous work [30]. In this experiment, the averaged center energies of electrons were 135 ± 20, 103 ± 14, and 78 ± 10 MeV at gas pressures of 33, 36, and 39 bar, respectively, with a charge of 300~600 pC per laser shoot. Typical electron spectra are shown in Figure 1. The bremsstrahlung γ-ray spectra were obtained by the average electron spectra of 100 continuous shots and GEANT4 simulations, which are also shown in Figure 1. The γ-ray intensities ($\geq$8 MeV) were $(1.60\pm 0.14)\times 10^8$, $(1.76\pm 0.13)\times 10^8$, and $(1.84\pm 0.11)\times 10^8$ per shoot at gas pressures of 33, 36, and 39 bar, respectively, the duration times were about 6.7 ps, which made the instantaneous intensities higher than 10^{19} S^{-1}.

2.2 Target

A laminated target made of 0.1mm ^{nat}Mo (99.99%), 0.1 mm ^{nat}Cu (99.99%), and 1 mm ^{27}Al (99.99%) was used for activation analysis in this experiment, all targets had a size of 2 × 2 cm. Some relative nuclear spectroscopic data of the radioactive nuclei from the Mo photonuclear reaction are shown in Table 1 [40]. The ^{65}Cu(γ, n) ^{64}Cu reaction (threshold energy at 9.91 MeV) and the ^{27}Al(γ, 2pn) ^{24}Na reaction (threshold energy at 31.45 MeV) were used as γ-ray flux monitors [15, 41]. The measurements of the FACSs of ^{65}Cu(γ, n) ^{64}Cu reaction and ^{27}Al(γ, 2pn)^{24}Na reaction directly reflected the accuracy of γ-ray spectrum. The repetition frequency was set at

TABLE 1 **Relative nuclear spectroscopic data of the radioactive nuclei from the Mo photonuclear reactions.**

Nucleus	Abundance (%)	Reaction	Half-life	Decay mode	Daughter nucleus	γ-ray energy	γ-ray branch
^{92}Mo	14.53	(γ, n)^{91m}Mo	64.6 s	IT 50.0%	^{91g}Mo	652.9	48.2%
				ϵ 50.0%	^{91}Nb	511	88%
						1,208.1	18.6%
						1,508.0	24.2%
		(γ, n)^{91g}Mo	15.49 m	ϵ 100%	^{91}Nb	511	187.48%
		(γ, 2n)^{90}Mo	5.56 h	ϵ 100%	^{90}Nb	511	50%
		(γ, 3n)^{89m}Mo	190 ms	IT 100%	^{89g}Mo	-	-
		(γ, 3n)^{89g}Mo	2.11 m	ϵ 100%	^{89}Nb	511	195%
						658.6	5.8%
						844.0	3.8%
		(γ, np)^{90}Nb	14.60 h	ϵ 100%	^{90}Zr	511	106%
^{98}Mo	24.39	(γ, p)^{97}Nb	72.1 m	β^- 100%	^{97}Mo	657.9	98.23%

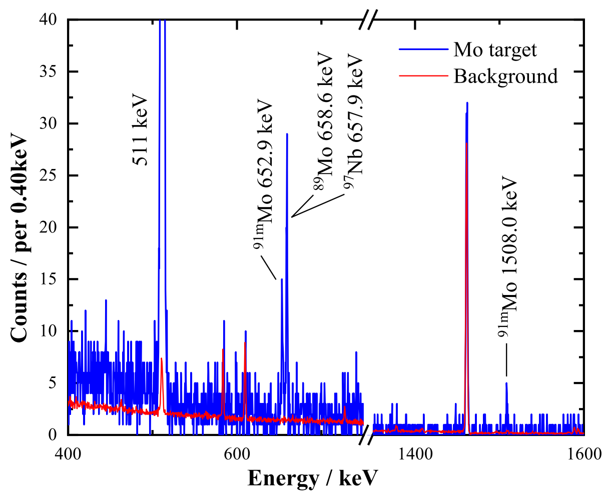

FIGURE 2
A typical spectrum of Mo target at gas pressure of 33 bar. The background spectrum measured for 5 h with a blank Mo target was also shown in the figure, the spectrum counts were normalized due to the living times.

0.2 Hz to keep the vacuum at acceptable levels. The irradiation time of each laminated target was 20 min for each electron energy.

2.3 Detector

Two HPGe detectors with a relative efficiency of 40% and a 3 × 3 inch $LaBr_3$ detector were used to measure activation signals after irradiation, all detectors were shielded in Pb brick. The detector efficiencies were calibrated using a standard ^{152}Eu source and a standard ^{60}Co source with an energy range of 121.8–1,408.0 keV, and were finally determined by GEANT4 simulations [42, 43]. The measuring of the Mo target started 1.5 min after the irradiation using a HPGe detector, the spectrum was saved every minute to analyze the decay characteristics and the total measuring time of each Mo target was 20 min. A typical activation spectrum of the Mo target with a measuring time of the first 3 min is shown in Figure 2.

3 Data analysis

As shown in Table 1 and Figure 2, the 652.9 and 1,508.0 keV γ-ray from ^{91m}Mo decay were clearly distinguished, but the 511 keV annihilation γ-ray of $\beta+$ decay can be produced in a variety of ways. The ^{90}Mo and ^{90}Nb have relatively long half-life times compared with ^{91m,g}Mo and ^{89g}Mo. Their contributions are relatively small due to the short irradiation time and can be regarded as a constant value during the short measuring time. The 511 keV signal of the background spectrum, as shown in Figure 2, is the combination of the $\beta+$ decay and the 510 keV γ-ray decay of ^{222}Rn in the environment, it was taken out as a constant value in our calculations. For the 568.6 keV γ-ray from ^{89g}Mo decay, it could not be distinguished from the 657.9 keV γ-ray from ^{97}Nb decay because of the similar energy. Meanwhile, the ^{89m}Mo could not be measured in this experiment due to its short half-life time of 190 ms. Therefore, the yields of ^{91m}Mo were determined by the 652.9 keV γ-ray and the yields of ^{91g}Mo and ^{89}Mo were determined by the 511 keV γ-ray.

The FACS $\sigma_{FA}(E)$ is defined as

$$\sigma_{FA}(E) = \frac{\int_{E_{thr}}^{E_{max}} \sigma(E)\varphi(E)dE}{\int_{E_{thr}}^{E_{max}} \varphi(E)dE} \tag{1}$$

where E_{thr} is the reaction threshold, $E_{\max}$ is the maximum energy of the γ-ray, $\sigma(E)$ is the energy-dependent reaction cross section, $\varphi(E)$ is the bremsstrahlung γ-ray flux. The reaction thresholds for the

TABLE 2 Experimental flux-weighted average cross sections of ^{92}Mo(γ, n) and (γ, 3n) reactions determined by present work and theoretical values of TALYS 1.9 calculated using a monoenergetic electron beam with the energies of 78, 103 and 135 MeV.

Reaction	Center energy of electrons	Experimental cross section	TALYS 1.9
	MeV	mb	mb
^{92}Mo(γ, n)$^{91m+g}$Mo	78 ± 10	33.7 ± 3.4	31.9
	103 ± 14	29.6 ± 3.3	28.2
	135 ± 20	26.5 ± 3.2	25.2
^{92}Mo(γ, n)^{91m}Mo	78 ± 10	17.4 ± 2.2	21.9
	103 ± 14	15.5 ± 2.1	19.2
	135 ± 20	13.6 ± 1.9	17.2
^{92}Mo(γ, n)^{91g}Mo	78 ± 10	16.3 ± 1.2	10.1
	103 ± 14	14.1 ± 1.2	8.9
	135 ± 20	12.9 ± 1.3	8.0
^{92}Mo(γ, 3n)$^{89m+g}$Mo	78 ± 10	0.291 ± 0.045	0.270
	103 ± 14	0.263 ± 0.042	0.221
	135 ± 20	0.231 ± 0.038	0.218

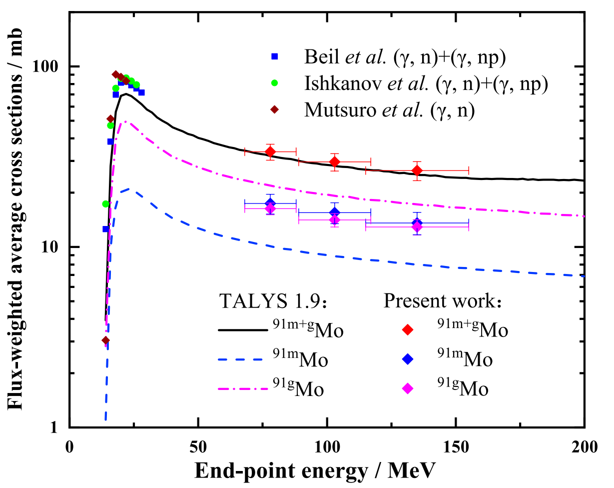

FIGURE 3
Experimental results of ^{92}Mo(γ, n)^{91m,g}Mo reaction FACSs, comparing with previous works [31–33] and TALYS 1.9 calculations.

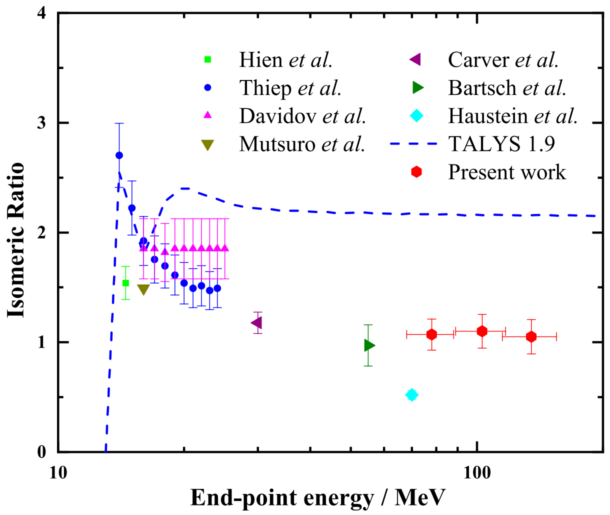

FIGURE 4
Experimental results of ^{92}Mo(γ, n)^{91m,g}Mo reaction IRs, comparing with previous works [31, 34–39] and TALYS 1.9 calculations.

productions of ^{91g}Mo, ^{91m}Mo, and ^{89}Mo are 12.67, 13.32, and 36.01 MeV, respectively. Then the FACS can be given by

$$\sigma_{FA}(E) = \frac{Y(E)}{N_0 \int_{E_{thr}}^{E_{max}} \varphi(E)dE} \tag{2}$$

where $Y(E)$ is the total yield, N_0 is the target nuclear number. The IR can be determined by

$$IR = \frac{\sigma_{FA}^m(E)}{\sigma_{FA}^g(E)} \tag{3}$$

where m and g stand for the parameters of isomeric state and ground state, respectively.

4 Results and discussion

The present FACSs and IRs are listed in Table 2 and shown in Figures 3, 4, 5 with comparisons of the previous works [31–39]. The statistical errors in this experiment range from 4.4% to 11.3% for different decay γ-ray, and the systematic errors include the instabilities of each electron pulse, the γ-ray spectrum calculation, the calibration of detection efficiency, and the correction of the activation target.

Theoretical values of the FACSs and IRs were calculated by GEANT4 simulation using the data from TENDL-2019 library

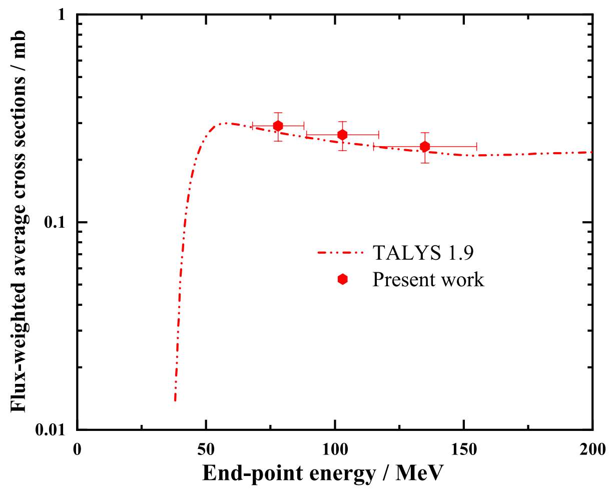

FIGURE 5
Experimental results of ^{92}Mo(γ, 3n)^{89}Mo reaction FACSs, comparing with TALYS 1.9 calculations.

[44] based on TALYS 1.9 code [45, 46], which were also shown in Tab. 2, Figure 3, Figure 4, and Figure 5.

For ^{92}Mo(γ, n)^{91m,g}Mo reaction, the total FACSs matched well with previous works. As shown in Figures 3, 4, the TALYS 1.9 calculation could not describe the reaction to the isomeric state or the ground state well, even though it gave a well-matched value of total cross sections. The TALYS 1.9 calculation underestimated the ^{92}Mo(γ, n)^{91g}Mo reaction cross sections by 38% at maximum while overestimated the ^{92}Mo(γ, n)^{91m}Mo reaction cross sections by 27% at maximum. The deviations between theory calculations and experiments might be caused by the inappropriate parameters of nuclear reaction model, nuclear level density, or optical potential, more theory calculations are stilled needed for this reaction. The IRs measured in this work matched well with the value of Bartsch *et al.* [38] within the uncertainties, the experimental discrepancies of ^{92}Mo(γ, n) ^{91m,g}Mo IRs were clarified. For ^{92}Mo(γ, 3n)^{89}Mo reaction, which is first achieved in this experiment, the TALYS 1.9 calculation described the FACSs very well.

5 Conclusion

The FACSs and IRs of ^{92}Mo(γ, n)^{91m,g}Mo reaction and ^{92}Mo(γ, 3n)^{89}Mo reaction were determined using laser-driven γ-ray by activation measurements. The experimental discrepancies of ^{92}Mo(γ, n)^{91m,g}Mo IRs at high energy region were clarified. However, we found thar the TALYS 1.9 code was not suitable for the production calculations of ^{92}Mo(γ, n) reaction, highlighting the need for more theoretical calculations. Additionally, the ^{92}Mo(γ, 3n)^{89}Mo reaction FACSs were achieved for the first time, filling in the gap of relevant experimental data.

Data availability statement

The original contributions presented in the study are included in the article/supplementary material, further inquiries can be directed to the corresponding author.

Author contributions

DW designed and preformed the experiment. DW, HL, and JZ analyzed the experimental data and performed TALYS and GEANT4 calculations. JL, JL, and HL performed the laser electron acceleration. XX and YG provided guidance on laser electron acceleration. HZ and YZ operated and optimized the laser machine. DW, HW, FL, and CH were involved in the activation measurement. JY, BG, NW, and XY provided investigations and resources for the experiment. XY was the supervisor of this work. DW wrote the first draft of the manuscript and HL and JL edited and contributed to sections of the manuscript. All authors contributed to the final editing and revision of the manuscript and approved it for submission.

Funding

This work was supported by the National Natural Science Foundation of China (Grants No. 11921006, 12125509), Beijing Outstanding Young Scientists Program, the National Grand Instrument Project (No. 2019YFF01014400), and the Open Foundation of Key Laboratory of High Power Laser and Physics, Chinese Academy of Sciences (No. SGKF202104).

Acknowledgments

The authors thank the staff of the 200 TW laser of CLAPA laboratory for the smooth operation of the machine.

Conflict of interest

The authors declare that the research was conducted in the absence of any commercial or financial relationships that could be construed as a potential conflict of interest.

The reviewer YS declared a shared affiliation with the authors HW, FL, BG, NW, and CH to the editor at the time of review.

Publisher's note

References

1. Tajima T, Dawson JM. Laser electron accelerator. *Phys Rev Lett* (1979) 43:267–70. doi:10.1103/PhysRevLett.43.267

2. Modena A, Najmudin Z, Dangor AE, Clayton CE, Marsh KA, Joshi C, et al. Electron acceleration from the breaking of relativistic plasma waves. *Nature* (1995) 377:606–8. doi:10.1038/377606a0

3. Faure J, Glinec Y, Pukhov A, Kiselev S, Gordienko S, Lefebvre E, et al. A laser–plasma accelerator producing monoenergetic electron beams. *Nature* (2004) 431:541–4. doi:10.1038/nature02963

4. Mangles S, Murphy C, Najmudin Z, Thomas A, Collier J, Dangor A, et al. Monoenergetic beams of relativistic electrons from intense laser–plasma interactions. *Nature* (2004) 431:535–8. doi:10.1038/nature02939

5. Geddes CGR, Toth CS, Tilborg JV, Esarey E, Schroeder CB, Bruhwiler D, et al. High-quality electron beams from a laser wakefield accelerator using plasma-channel guiding. *Nature* (2004) 431:538–41. doi:10.1038/nature02900

6. Pukhov A, ter Vehn JM. Laser wake field acceleration: The highly non-linear broken-wave regime. *Appl Phys B* (2002) 74:355–61. doi:10.1007/s003400200795

7. Lu W, Huang C, Zhou M, Mori WB, Katsouleas T. Nonlinear theory for relativistic plasma wakefields in the blowout regime. *Phys Rev Lett* (2006) 96:165002. doi:10.1103/PhysRevLett.96.165002

8. Giulietti A, Bourgeois N, Ceccotti T, Davoine X, Dobosz S, D'Oliveira P, et al. Intense γ-ray source in the giant-dipole-resonance range driven by 10-tw laser pulses. *Phys Rev Lett* (2008) 101:105002. doi:10.1103/PhysRevLett.101.105002

9. Ferri J, Corde S, Döpp A, Lifschitz A, Doche A, Thaury C, et al. High-brilliance betatron γ-ray source powered by laser-accelerated electrons. *Phys Rev Lett* (2018) 120: 254802. doi:10.1103/PhysRevLett.120.254802

10. Li S, Shen BF, Xu JC, Xu TJ, Yu Y, Li JF, et al. Ultrafast multi-mev gamma-ray beam produced by laser-accelerated electrons. *Phys Plasmas* (2017) 24:093104. doi:10.1063/1.4996020

11. Döpp A, Guillaume E, Thaury C, Lifschitz A, Sylla F, Goddet JP, et al. A bremsstrahlung gamma-ray source based on stable ionization injection of electrons into a laser wakefield accelerator. *Nucl Instr Methods Phys Res Section A* (2016) 830: 515–9. doi:10.1016/j.nima.2016.01.086

12. Tanaka KA, Spohr KM, Balabanski DL, Balascuta S, Capponi L, Cernaianu MO, et al. Current status and highlights of the ELI-NP research program. *Matter Radiat Extremes* (2020) 5:024402. doi:10.1063/1.5093535

13. An GP, Chi YL, Dang YL, Fu GY, Guo B, Huang YS, et al. High energy and high brightness laser compton backscattering gamma-ray source at IHEP. *Matter Radiat Extremes* (2018) 3:219–26. doi:10.1016/j.mre.2018.01.005

14. Wang HW, Fan GT, Liu LX, Xu HH, Shen WQ, Ma YG, et al. Commissioning of laser electron gamma beamline SLEGS at SSRF. *Nucl Sci Tech* (2022) 33:87. doi:10.1007/s41365-022-01076-0

15. Naik H, Kim G, Kim K, Zaman M, Goswami A, Lee MW, et al. Measurement of flux-weighted average cross sections for ^{197}Au(γ, xn) reactions and isomeric yield ratios of ^{196m,g}Au with bremsstrahlung. *Nucl Phys A* (2016) 948:28–45. doi:10.1016/j.nuclphysa.2016.01.015

16. Boller P, Zylstra A, Burggraf J, Henry G, Bernstein L, Brabetz C, et al. *Nuclear excitation and fission studies with short pulsed laser-driven high energy gamma rays*. Livermore, CA, United States: Lawrence Livermore National Lab. (2021). Technical report.

17. Ma Z, Lan H, Liu W, Wu S, Xu Y, Zhu Z, et al. The role of angular-momentum removal in photonuclear reactions as deduced from the isomeric ratios for ^{120m,g}Sb and ^{117m,g}In. *J Phys G Nucl Part Phys* (1998) 24:589. doi:10.1088/0954-3899/24/3/010

18. Boyer K, Luk T, Rhodes C. Possibility of optically induced nuclear fission. *Phys Rev Lett* (1988) 60:557–60. doi:10.1103/PhysRevLett.60.557

19. Mirani F, Calzolari D, Formenti A, Passoni M. Superintense laser-driven photon activation analysis. *Commun Phys* (2021) 4:185–13. doi:10.1038/s42005-021-00685-2

20. Vandenbosch R, Huizenga JR. Isomeric cross-section ratios for reactions producing the isomeric pair Hg197,197m. *Phys Rev* (1960) 120:1313–8. doi:10.1103/PhysRev.120.1313

21. Huizenga JR, Vandenbosch R. Interpretation of isomeric cross-section ratios for (n, γ) and (γ,n) reactions. *Phys Rev* (1960) 120:1305–12. doi:10.1103/PhysRev.120.1305

22. Blann M. Preequilibrium decay. *Annu Rev Nucl Part Sci* (1975) 25:123–66. doi:10.1146/annurev.ns.25.120175.001011

23. Tsoneva N, Stoyanov C, Gangrsky YP, Ponomarev VY, Balabanov NP, Tonchev AP. Population of isomers in the decay of the giant dipole resonance. *Phys Rev C* (1999) 61:044303–555. doi:10.1103/PhysRevC.61.044303

24. Kolev D, Ernest J, Liu W, Wu S, Xu Y, Zhu Z, et al. Photonuclear production of medical isotopes ^{62,64}Cu using intense laser-plasma electron source. *Matter Radiat Extremes* (2019) 4:064401. doi:10.1063/1.5100925

25. Burbidge EM, Burbidge GR, Fowler WA, Hoyle F. Synthesis of the elements in stars. *Rev Mod Phys* (1957) 29:547–650. doi:10.1103/RevModPhys.29.547

26. Arnould M, Goriely S. The p-process of stellar nucleosynthesis: Astrophysics and nuclear physics status. *Phys Rep* (2003) 384:1–84. doi:10.1016/S0370-1573(03)00242-4

27. Sauerwein A, Elvers M, Endres J, Hasper J, Hennig A, Netterdon L, et al. Nuclear physics experiments for the astrophysical *p* process. *Prog Part Nucl Phys* (2011) 66: 363–7. doi:10.1016/j.ppnp.2011.01.035

28. Rauscher T, Dauphas N, Dillmann I, Fröhlich C, Fülöp Z, Gyürky G. Constraining the astrophysical origin of the p-nuclei through nuclear physics and meteoritic dataöhlich C, Fülöp Z, Gyürky G. Constraining the astrophysical origin of the *p*-nuclei through nuclear physics and meteoritic data. *Rep Prog Phys* (2013) 76: 066201. doi:10.1088/0034-4885/76/6/066201

29. Rapp W, Gorres J, Kappeler F. Sensitivity of*p*-Process Nucleosynthesis to Nuclear Reaction Rates in a 25$M_{\odot}$Supernova Modelörres1 J, Wiescher M, Schatz H, K$\ddot {a}$ppeler F. Sensitivity of p-process nucleosynthesis to nuclear reaction rates in a 25 $m_{\odot}$ supernova model. *Astrophysical J* (2006) 653:474–89. doi:10.1086/508402

30. Wu D, Zhang J, Lan H, Liu J, Lv J, Lu H, et al. ^{197}Au(γ, *xn*; x = 1~7) reaction measurements using laser-driven ultra-bright ultra-fast bremsstrahlung γ-ray. arXiv: 2209.13947v1 [nucl–ex] (2022).

31. Mutsuro N, Ohnuki Y, Sato K, Kimura M. Photo-neutron cross sections for ^{107}Ag, ^{92}Mo and ^{90}Zr. *J Phys Soc Jpn* (1959) 14:1649–53. doi:10.1143/JPSJ.14.1649

32. Bsishkhanov I, Evlazutin I, Opshevchenko. Intermediate structure of the cross sections of photoneutron reactions on the isotopes of Mo. *Soviet J Nucl Phys* (1970) 11:702.

33. Beil H, Bergère R, Carlos P, Leprêtre A, De Miniac A, Veyssière A. A study of the photoneutron contribution to the giant dipole resonance in doubly even mo isotopes. *Nucl Phys A* (1974) 227:427–49. doi:10.1016/0375-9474(74)90769-6

34. Carver JH, Coote GE, Sherwood TR. Isomeric (γ,n) cross section ratios and the spin dependence of the nuclear level density. *Nucl Phys* (1962) 37:449–56. doi:10.1016/0029-5582(62)90277-8

35. Haustein PE, Voigt AF. Isomer ratio measurements for ^{91}Mo, ^{137}Ce and ^{141}Nd produced by (γ,n) and (γ, 3n) reactions. *J Inorg Nucl Chem* (1971) 33:289–94. doi:10.1016/0022-1902(71)80368-8

36. Khien FZ, Zui NQ, An NT. Study of isomer ratio in (n,2n) and (γ,n) reactions on 92Mo,^{90}Zr,86Sr and ^{74}Se. *Soviet J Nucl Phys* (1982) 35:257.

37. Davydov MG, Magera VG, Trukhov AV. Isomeric ratios of the yields (cross sections) of photonuclear reactions. *Soviet At Energ* (1987) 62:277–85. doi:10.1007/bf01123367

38. Bartsch H, Huber K, Kneissl U, Krieger H. Critical consideration of the statistical model analysis of photonuclear isomeric cross-section ratios. *Nucl Phys A* (2016) 256: 243–52. doi:10.1016/0375-9474(76)90106-8

39. Thiep TD, An TT, Cuong PV, Vinh NT, Hue BM, Belov AG, et al. Isomeric ratios in photonuclear reactions of molybdenum isotopes induced by bremsstrahlung in the giant dipole resonance region. *Phys Particles Nuclei Lett* (2017) 14:102–11. doi:10.1134/S1547477117010241

40. Nudat 3.0. National nuclear data center (2022).

41. Naik H, Singh S, Goswami A, Manchanda VK, Kim G, Kim KS, et al. Measurement of photo-neutron cross-sections in 208pb and 209bi with 50–70mev bremsstrahlung. *Nucl Instr Methods Phys Res Section B: Beam Interactions Mater Atoms* (2011) 269:1417–24. doi:10.1016/j.nimb.2011.04.008

42. Agostinelli S, Allison J, Amako K, Apostolakis J, Araujo H, Arce P, et al. Geant4—A simulation toolkit. *Nucl Instr Methods Phys Res Section A* (2003) 506: 250–303. doi:10.1016/S0168-9002(03)01368-8

43. Allison J, Amako K, Apostolakis J, Araujo H, Dubois P, Asai M, et al. Geant4 developments and applications. *IEEE Trans Nucl Sci* (2006) 53:270–8. doi:10.1109/TNS.2006.869826

44. Koning A, Rochman D, Sublet J, Dzysiuk N, Fleming M, van der Marck S. Tendl: Complete nuclear data library for innovative nuclear science and technology. *Nucl Data Sheets* (2019) 155:1–55. doi:10.1016/j.nds.2019.01.002

45. Koning A, Rochman D. Modern nuclear data evaluation with the talys code system. *Nucl Data Sheets* (2012) 133:2841–934. doi:10.1016/j.nds.2012.11.002

46. Alhassan E, Rochman D, Vasiliev A, Hursin M, Koning AJ, Ferroukhi H. Iterative bayesian Monte Carlo for nuclear data evaluation. *Nucl Sci Tech* (2022) 33:50. doi:10.1007/s41365-022-01034-w